Influence of coherent optical phonon on ultrafast energy relaxation

J. L. Wang,[1,a)] L. Guo,[2] C. H. Liu,[1] X. Xu,[2,a)] and Y. F. Chen[1]
[1]*Jiangsu Key Laboratory for Design and Manufacture of Micro/Nano Biomedical Instruments, Southeast University, Nanjing 210096, China*
[2]*School of Mechanical Engineering and Birck Nanotechnology Center, Purdue University, West Lafayette, Indiana 47907, USA*

(Received 8 April 2015; accepted 30 July 2015; published online 13 August 2015)

Ultrafast energy relaxation process in Bi_2Te_3 thin films is studied using a collinear two color pump-probe technique. The coherent optical phonon is enhanced and destroyed by changing the separation times of double pump pulses. The non-oscillatory component of the reflectivity trace after the second pump pulse shows a distinct difference with and without the presence of coherent optical phonons, thus providing a direct evidence of the effect of optical phonon on the hot carrier relaxation process. The deduced characteristic times are systematically smaller when coherent optical phonons are involved in the energy transfer process. Comparatively, the conventional relaxation process is relatively slow, which is explained by the screening effect of the incoherent optical phonon. This work suggests that the energy relaxation can be manipulated through the excitation of coherent optical phonons. © *2015 AIP Publishing LLC*. [http://dx.doi.org/10.1063/1.4928657]

Ultrafast spectroscopy has been widely used to study the carrier and phonon dynamics in semiconductors.[1] In general, the photo-exited carriers first interact among themselves to redistribute energy and momentum, then cool down to the lattice subsystem through different mechanisms, including coupling among carriers, optical phonons (OPs), and acoustic phonons (APs), as well as spatial evolution of carriers and phonons. The rise and fall of the transient reflectance are usually complicated, and there is still a lack of consistency in the interpretations.[2–6] The photo-excited carriers also change the equilibrium position of the atoms instantaneously.[7] If the pulse duration is shorter than the periods of atomic vibrations, atoms can oscillate around their new equilibrium position collectively, which is referred to as coherent OP. Excitation and detection of coherent OP provide an important insight into the lifetimes of phonons and interactions with excited carriers, which are essential processes for a number of interesting phenomena such as non-thermal melting[8] and insulator-to-metal transition.[9] The excited coherent OP is distinct in some semiconductors, such as Bi,[10] Bi_2Se_3,[11] and Bi_2Te_3,[12] and its damping rate is associated with the relaxation process through interactions with longitudinal optical phonons (L-OPs) and APs. Since OP mediates carrier-phonon energy exchange,[13] it is reasonable to anticipate that the coherent OP can affect the non-oscillatory component in transient reflectance, which is rarely reported in literature.[14]

In this experiment, p-type Bi_2Te_3 single crystalline films were synthesized by metalorganic chemical vapor deposition on a (100) GaAs substrate with thickness of about 50 nm, which is much thicker than the absorption depth (~10 nm) at the 400 nm pump laser wavelength. The temporal reflectivity was measured in a collinear two-color (800 and 400 nm) pump-probe scheme, and the details of the setup can be found in Ref. 12. The experiments were carried out at low temperature (80 K) to prolong the coherent OPs. A pulse shaper (MIIPS Box 640) was used in the pump arm to generate double-pulse trains. To avoid heating damage, the pump fluence of about 80 $\mu J/cm^2$ was maintained throughout the experiments. The band gap of Bi_2Te_3 at 80 K is calculated to be about 0.15 eV;[15] the carrier density is estimated to be about 2×10^{21} cm^{-3};[16] the corresponding peak electron temperature is about 490 K;[17] and the energy density at the end of pump pulse is about 0.05 kJ/cm^3,[16] which is far below the enthalpy of fusion (1.1 kJ/cm^3) of Bi_2Te_3.[18]

Figure 1 shows the temporal evolution of the transient reflectivity changes, $\Delta R/R$. Negative differential reflectivity is obtained due to the absorption bleaching.[19] The reflectivity trace consists of oscillatory and non-oscillatory components. The slow and fast oscillations are attributed to the coherent AP and coherent OP,[6] respectively. The damped oscillatory function is used to characterize the high-frequency oscillatory component

$$R_{osc} = A_{op} e^{-t/t_{op}} \cos(2\pi f t + \varphi), \quad (1)$$

with $f = 1.9$ THz and $t_{op} = 11.9$ ps, which agree well with the previous reported values.[20] The coherent AP with a lower frequency of about 0.04 THz appears when the delay is longer than 20 ps. The coherent AP is contributed to the strain pulse propagation,[21] which gives rise to the peak 3 in Figure 1(a). The oscillation frequency of coherent AP can be estimated by $f = 2nv/\lambda$, where n is the refractive index (~4.5),[22] v is the sound velocity (~2500 m/s),[23] and λ is the wavelength of the probe (800 nm). The predicted value is about 0.03 THz, which is close to the experimental data. Compared with the oscillatory part, the non-oscillatory component is more complicated, the trace has a sharp increase after pump pulse excitation within a time duration of less than 1 ps (period I), subsequently decreases in a couple of ps (period II), then rises again to reach a peak value (peak 2) at about 12 ps (period III), and finally decays slowly back to the background (period IV), which is much longer than the time

[a)]Authors to whom correspondence should be addressed. Electronic addresses: wangjianli@seu.edu.cn and xxu@ecn.purdue.edu

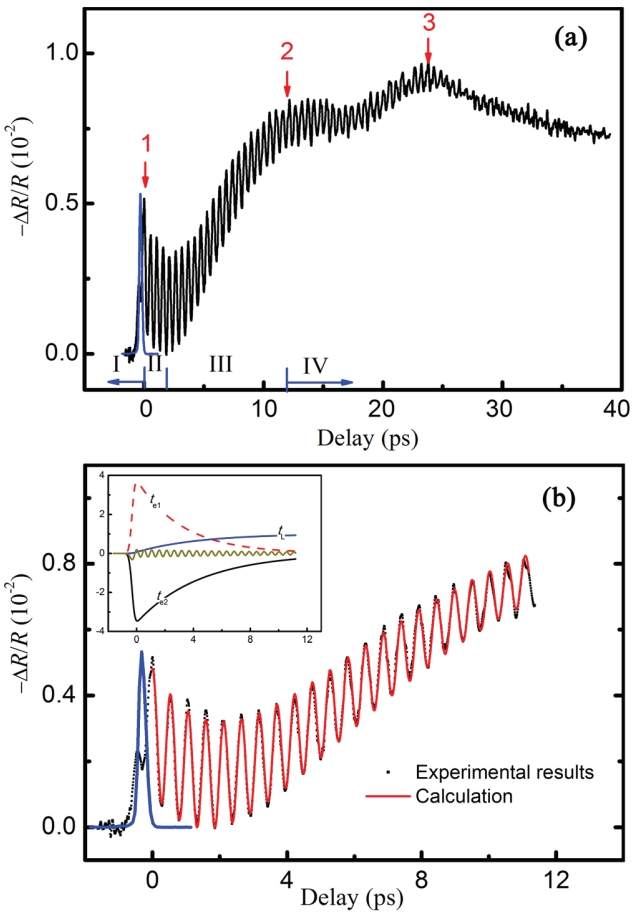

FIG. 1. (a) Temporal evolution of reflectivity trace (black) for 50 nm Bi_2Te_3 nanofilms measured at 80 K. The cross-correlation of the pump and the probe pulses (blue) is shown as a reference. (b) Fitting result of the first few ps data is obtained by using the phenomenological model. The inset shows the contributions from each component with different time constants.

window shown. Hot carries are photo-excited in period I, when the momentum relaxation and Coulomb thermalization occur at a timescale of tens of fs.[1] The slow decay in period IV can be explained by the carrier recombination and diffusion, and the corresponding characteristic time is over hundreds of ps.[1] Comparatively, the carrier and the phonon dynamics occurring in periods II and III are not fully understood, therefore are the focus of the present study.

Similar to the observations in Bi_2Se_3,[3] the process in period II is due to the relaxation of carrier density, caused by carrier-phonon scattering and carrier diffusion, and the rise after around 2 ps (period III) reflects the lattice heating effect.[14,24] Generally, thermalization from hot carriers to L-OP occurs in less than few ps,[25] much faster than that from hot carriers to AP, and the Fröhlich interaction dominates the carrier-phonon scattering process. In this case, the hot carriers first emit OP and then decay to lower energy phonon mode (AP).[6] The energy relaxation from OP to AP is mainly through the anharmonic effect, which slows down at low temperature (t_{op} is about two times larger than that at room temperature),[20] so the distribution of OP is driven substantially out of equilibrium. The non-equilibrium OP has been extensively studied, which can dramatically reduce the cooling rate of the carriers especially at high carrier density.[6,25,26] In view of the non-equilibrium incoherent OP, the two-temperature model,[27] which solely considers the electron and the lattice temperatures, is inadequate to describe the physical processes. Here, we adopted a phenomenological model to analyze the transient process in periods II and III

$$R_{\mathrm{mon}} = A_{e1}e^{-t/t_{e1}} + A_{e2}e^{-t/t_{e2}} + A_L(1 - e^{-t/t_L}), \qquad (2)$$

where the sum of the first two terms accounts for the reflectivity response due to the interaction between carriers and OPs, and the third term represents lattice heating. For the first two terms, the amplitudes A_{e1} and A_{e2} have opposite signs, and the decay rates are also different. Similar results were observed in other semiconductors,[2,5,6,11,24,28] which are possibly associated with the carrier trapping effect,[2] hot phonon relaxation,[6] or different groups of carriers.[5] The overall response is expressed by the convolution[17]

$$\frac{\Delta R}{R} = (R_{\mathrm{osc}} + R_{\mathrm{mon}})U(t + t_0) \otimes G, \qquad (3)$$

where $U(t+t_0)$ is the unit step function, G is the cross-correlation of the pump and the probe pulses. The peak 1 is set as the zero time reference in Figure 1(a), so t_0 is introduced to reflect the arrival of the pump pulse, which is found to be 0.32 ps. G is represented by a Gaussian function, i.e., $G = e^{-2(t/\sigma)^2}$, and σ is the full width at half maximum (FWHM) of cross-correlation, which is found to be about 260 fs. The solid curve in Figure 1(b) shows a good fit, and the contribution from each component is plotted in the inset. It is worth noting that t_{e2} and t_L are almost equal at 80 K ($t_{e2} \approx t_L \sim 4.4$ ps); in this case, Eq. (2) can be reduced to the formula proposed in other works.[5,29] This coincidence implies that the coupling between A_{e2} component and lattice heating can be relatively stronger compared with the fast decay carrier component ($t_{e1} \approx 3.1$ ps).

Although the phenomenological models have been widely used to fit the reflectivity traces,[2,5,11,14,24,28,29] the interpretation of each component in Eq. (2) lacks consistency, especially for the slow decay component of carriers (A_{e2}), which is sometimes ascribed to the carrier-AP interaction.[5] Understanding the role of OP on energy transport process is significantly important in solving these disputes, however, it is hard to provide a direct evidence of strong coupling between the experimental reflectivity data and OPs, and the generation and relaxation of incoherent OP has been used to explain the different decay rate of hot carriers.[6] In general, the incoherent OPs are created during the carrier cooling process. Comparatively, if the generation of coherent OP is considered as a process of the Displacive Excitation of Coherent Phonon (DECP),[7] the coherent OPs are generated almost simultaneously along with the hot carriers. The A_{1g} mode (L-OP) is distinct in the reflectivity traces, which is likely to affect the energy relaxation process. In our work, by carefully adjusting the intensity and separation time between the two successive pump pulses, the coherent OPs are completely cancelled or enhanced, as shown in Figure 2(a). The oscillation period T is found to be 0.528 ps; therefore, the

separation times for cancellation and enhancement are set to 1.848 ps (3.5 T) and 1.584 ps (3 T), respectively. The arrival of the second pump pulse is one of the primary concerns in our experiment. To make a good comparison in periods II and III, the second pump pulses are set to arrive at sample surface simultaneously, which can be further verified by the cross-correlation signals (Figure 2(a)). The energy of the pump and the probe pulses used in these experiments is fixed. Furthermore, since the pump energy eventually transfers to the lattice subsystem, the overlap of signals at long delay times (after tens of ps) can also justify that the same pump fluence is used in the experiments, as shown in Figure 2(a). To identify the difference between the non-oscillatory components in the two curves in Figure 2(a), the change in the differential reflectivity is introduced, defined by $DR = (\Delta R/R)_{3.5T} - (\Delta R/R)_{3T}$, which is shown in the red curve in Figure 2(b). Two symmetric exponential-decay curves (dashed blue lines) are also plotted to guide the eye. The background signals before the arrival of the first pump pulse are overlapped for the same pump fluences, so the background subtraction will not introduce artificial difference in Figure 2(b). It is found that, the positive component in the DR curve is larger than the negative one for the first 20 ps or so, and afterwards, the difference gradually disappears. To further estimate the effect of the carrier delay response induced by the first pump pulse, the enhancement and cancellation results are simulated based on the signal detected by the single pump-pulse illumination (Figure 1(b)), and the corresponding DR after the second pump pulse is shown in the black curve in Figure 2(b) as a comparison. The positive component in the simulated DR curve is nearly symmetric with the negative one; thus, the carrier delay response is not likely to induce this asymmetric behavior.

We again applied the phenomenological model to fit the non-oscillatory component in the reflectivity traces with and without the coherent OP. In the double-pump experiments, t_0 in the unit step function is set to $t_0 = (t_s + 0.32)$ ps, where t_s is the inter-pump delay and

$$G = \frac{P}{1+P} e^{-2\left(\frac{t+t_s}{\sigma}\right)^2} + \frac{1}{1+P} e^{-2\left(\frac{t}{\sigma}\right)^2}. \quad (4)$$

In order to completely cancel the coherent OP when $t_s = 3.5\,T$, P is found to be 1.175. The least-square method was used to fit the experimental data after the second pump pulse, and the results are shown in solid curves in Figure 3(a), with the fitting parameters listed in Table I. To confirm the findings, we measured the same sample with relatively smaller pump fluence at separation times of 2 T, 2.5 T, and 3 T, and the experimental and fitting results are shown in

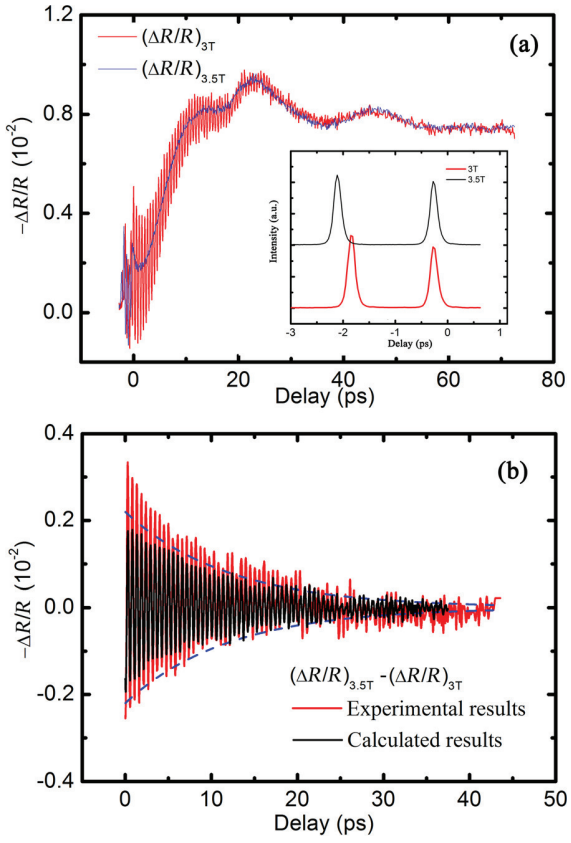

FIG. 2. (a) Temporal evolution of reflectivity traces pumped by a double-pulse trains with separation times of 3 T ($T = 0.528$ ps, red line) and 3.5 T (blue line). The inset shows the corresponding cross-correlation curves. (b) Comparison of difference in the reflectivity change, $DR = (\Delta R/R)_{3.5T} - (\Delta R/R)_{3T}$, obtained by experimental data (red curve) and simulated results (black curve); two symmetric exponential decay curves (dashed blue lines) are presented to guide the eye.

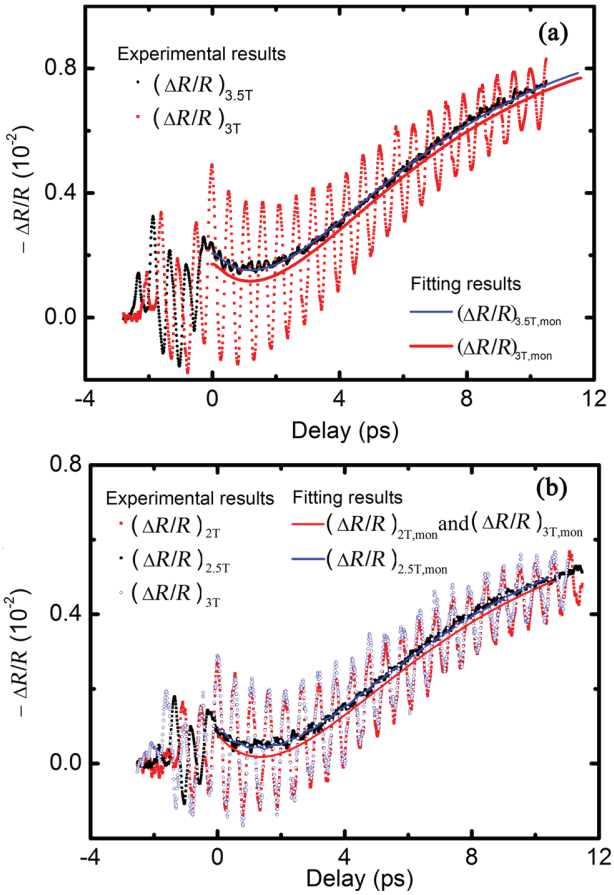

FIG. 3. (a) Temporal evolution of reflectivity traces with and without coherent OP, the corresponding non-oscillatory components after the second pump pulse are fitted by the phenomenological model. (b) Experimental and fitting results obtained at separation times of 2 T, 2.5 T, and 3 T with relatively smaller pump fluence.

TABLE I. Summary of fitting values.

Separation time (ps)	A_{e1} (10^{-2})	t_{e1} (ps)	A_{e2} (10^{-2})	t_{e2} (ps)	$A_L(10^{-2})$	t_L (ps)
1.584	9.89	2.95	−9.1	4.21	2.32	4.20
1.848	10.0	3.00	−9.0	4.40	2.43	4.41

Figure 3(b). It is found that the data measured at $2T$ and $3T$ after the second pump pulse are almost the same, while the non-oscillatory components with and without the coherent OP are different. The difference in the two curves right after the second pump pulse corresponds to lower photo-excited carrier density in the coherent OP enhancement case, since a part of carrier energy transfers directly to the coherent OP, resulting in smaller absolute values of amplitudes (A_{e1} and A_{e2}). Moreover, the decay times of electron relaxation (t_{e1} and t_{e2}) are different with the presence of the coherent OP, indicating that the first two terms in Eq. (2) are possibly both affected by the relaxation of carriers via OPs. The effect of the coherent OP on various groups of carriers[5] is different, and the change in the slow decay component (A_{e2}) is more obvious. The decay times (t_{e1} and t_{e2}) in $(\Delta R/R)_{3T}$ are smaller than those in $(\Delta R/R)_{3.5T}$, revealing that the energy transfers more efficiently through coherent OP to lattice subsystem compared with the conventional process in which incoherent OP mediates the carrier-phonon energy exchange.

DeCamp *et al.*[30] provided that a 0.1% relative change in reflectivity trace corresponded to a displacement of about 10^{-3} Å. In the DECP model,[7] the displacement depends linearly on the pump fluence, so does the amplitude of coherent vibration.[12] It is hence reasonable to anticipate that the displacement is proportional to the amplitude of coherent vibration. Based on this approximation, in the coherent OP enhancement case, the maximum displacements after the arrival of the first and the second pump pulses are estimated to be 2.2×10^{-3} Å and 3.05×10^{-3} Å, respectively, and the displacement induced by the first pump pulse decays exponentially to 1.93×10^{-3} Å at the arrival of the second pump pulse. We employed the density functional theory in the Vienna *Ab initio* Simulation Package (VASP)[31] to calculate the energy coupled to the coherent OP after the second pump pulse. Figure 4 shows the computed results of energy per unit cell as a function of displacement when the two pairs of Bi and Te1 atoms are stretched from each other along the c-axis (A_{1g} mode). Then, the energy coupled to the coherent OP can be calculated by

$$E_{C\text{-}OP} = \frac{E_2 - E_1}{V_c} V, \tag{5}$$

where E_1 and E_2 are the energy per unit cell for displacement at 1.93×10^{-3} Å and 3.05×10^{-3} Å, V_c is the volume of the primitive unit cell, $V_c \sim 169.11$ Å^3, V is the absorption volume, which can be estimated by $V = \pi d^2 \delta/4$, d is the spot diameter, and δ is the absorption depth. Finally, $E_{C\text{-}OP}$ is found to be about 6.7×10^{-11} J, which accounts for about 12% of the absorbed energy of the second pump pulse. In this calculation, the absorbed energy from the second pump pulse is calculated by $E_{ab} = \pi \alpha F d^2/4/(1+P)$, where F is the fluence of pump pulse (80 μJ/cm^2), α is the absorptivity ($\sim$0.3),[16] so E_{ab} is found to be about 5.7×10^{-10} J.

In summary, we investigated ultrafast energy transfer process in Bi_2Te_3 thin films through enhancing and cancelling the coherent OP using two pump pulses with different separation times. With the presence of the coherent OP, the non-oscillatory component of the reflectivity trace was different from the other case when the coherent OP was completely cancelled, and smaller characteristic times were obtained, indicating more efficient energy transfer rate compared with the normal processes when the incoherent OP mediates the carrier-phonon energy exchange.

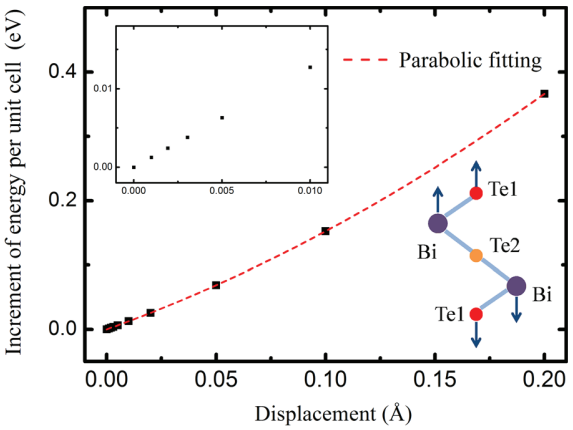

FIG. 4. Calculated energy per unit cell over large (main panel) and small (inset panel) displacements. The inset shows the coherent A_{1g} mode.

This work was supported by the National Science of Foundation Award No. 1048616, the Department of Energy through a Corporate Agreement No. DE-AC05000OR22725 with General Motors R&D, the National Basic Research Program of China (Grant No. 2011CB707605), and the National Natural Science Foundation of China (Grant No. 51476033).

[1]A. Othonos, Appl. Phys. Rev. **83**, 1789 (1998).
[2]P. Grenier and J. F. Whitaker, Appl. Phys. Lett. **70**, 1998 (1997).
[3]N. Kumar, B. A. Ruzicka, N. P. Butch, P. Syers, K. Kirshenbaum, J. Paglione, and H. Zhao, Phys. Rev. B **83**, 235306 (2011).
[4]M. A. M. Versteegh, T. Kuis, H. T. C. Stoof, and J. I. Dijkhuis, Phys. Rev. B **84**, 035207 (2011).
[5]A. A. Melnikov, O. V. Miscochko, and S. V. Chekalin, J. Appl. Phys. **114**, 033502 (2013).
[6]Y. P. Lai, H. J. Chen, K. H. Wu, and J. M. Liu, Appl. Phys. Lett. **105**, 232110 (2014).
[7]H. J. Zeiger, J. Vidal, T. K. Cheng, E. P. Ippen, G. Dresselhaus, and M. S. Dresselhaus, Phys. Rev. B **45**, 768 (1992).
[8]A. Rousse, C. Rischel, S. Fourmaux, I. Uchmann, S. Sebban, G. Grillon, Ph. Balcou, E. Förster, J. P. Geindre, P. Audebert, J. C. Gauthler, and D. Hulin, Nature **410**, 65 (2000).
[9]M. Chollet, L. Cuerin, N. Uchida, S. Fukaya, H. Shimoda, T. Ishikawa, K. Matsuda, T. Hasegawa, A. Ota, H. Yamochi, G. Saito, R. Tazaki, S.-I. Adachi, and S.-Y. Koshihara, Science **307**, 86 (2005).
[10]T. K. Cheng, J. Vidal, H. J. Zeiger, G. Dresselhaus, M. S. Dresselhaus, and E. P. Ippen, Appl. Phys. Lett. **59**(16), 1923 (1991).
[11]J. Qi, X. Chen, W. Yu, P. Cadden-Zimansky, D. Smirnov, N. H. Tolk, I. Miotkowski, H. Cao, Y. P. Chen, Y. Wu, S. Qiao, and Z. Jiang, Appl. Phys. Lett. **97**, 182102 (2010).
[12]A. Q. Wu, X. F. Xu, and R. Venkatasubramanian, Appl. Phys. Lett. **92**, 011108 (2008).

[13]A. R. Vasconcellos and R. Luzzi, J. Phys. Chem. Solids **45**, 191 (1984).
[14]A. Q. Wu and X. F. Xu, Appl. Phys. Lett. **90**, 251111 (2007).
[15]I. G. Austin, Proc. Phys. Soc. London **72**, 545 (1958).
[16]E. G. Gamaly, Phys. Rep. **508**, 91 (2011).
[17]Y. G. Wang, L. Guo, X. F. Xu, J. Pierce, and R. Venkatasubramanian, Phys. Rev. B **88**, 064307 (2013).
[18]N. P. Gorbachuk and V. R. Sidorko, Powder Metal. Met. Ceram. **43**, 284 (2004).
[19]Y. D. Glinka, S. Babakiray, T. A. Johnson, A. D. Bristow, M. B. Holcomb, and D. Lederman, Appl. Phys. Lett. **103**, 151903 (2013).
[20]N. Kamaraju, S. Kumar, and A. K. Sood, EPL **92**, 47007 (2010).
[21]C. Thomsen, H. T. Grahn, H. J. Maris, and J. Tauc, Phys. Rev B **34**, 4129 (1986).
[22]H. Cui, I. B. Bhat, and R. Venkatasubramanian, J. Electron. Mater. **28**, 1111 (1999).
[23]Y. G. Wang, B. Qiu, A. J. H. McGaughey, X. Ruan, and X. F. Xu, J. Heat Transfer **135**, 091102 (2013).
[24]L. Jia, W. G. Ma, and X. Zhang, Appl. Phys. Lett. **104**, 241911 (2014).
[25]P. A. Maksym, J. Phys. C: Solid State Phys. **15**, 3127 (1982).
[26]H. M. van Driel, Phys. Rev. B **19**, 5928 (1979).
[27]L. Guo, S. L. Hodson, T. S. Fisher, and X. F. Xu, J. Heat Transfer **134**, 042402 (2012).
[28]Y. D. Glinka, N. H. Tolk, X. Liu, Y. Sasaki, and J. K. Furdyna, J. Appl. Phys. **103**, 043708 (2008).
[29]Y. Xu, M. Khafizov, L. Satrapinsky, P. Kúš, A. Plecenik, and R. Sobolewski, Phys. Rev. Lett. **91**, 197004 (2003).
[30]M. F. DeCamp, D. A. Reis, P. H. Bucksbaum, and R. Merlin, Phys. Rev. B **64**, 092301 (2001).
[31]G. Kresse and J. Furthmuller, Comput. Mater. Sci. **6**, 15 (1996).